



UNIVERSITÀ
DEGLI STUDI
FIRENZE

FLORE

Repository istituzionale dell'Università degli Studi di Firenze

Determining calcium carbonate reaction kinetics from experimental laboratory data

Questa è la Versione finale referata (Post print/Accepted manuscript) della seguente pubblicazione:

Original Citation:

Determining calcium carbonate reaction kinetics from experimental laboratory data / L.Fusi; A.Monti; M.Primicerio. - In: JOURNAL OF MATHEMATICAL CHEMISTRY. - ISSN 0259-9791. - STAMPA. - 50:(2012), pp. 2492-2511. [10.1007/s10910-012-0045-3]

Availability:

This version is available at: 2158/793991 since:

Published version:

DOI: 10.1007/s10910-012-0045-3

Terms of use:

Open Access

La pubblicazione è resa disponibile sotto le norme e i termini della licenza di deposito, secondo quanto stabilito dalla Policy per l'accesso aperto dell'Università degli Studi di Firenze (<https://www.sba.unifi.it/upload/policy-oa-2016-1.pdf>)

Publisher copyright claim:

(Article begins on next page)

Determining calcium carbonate neutralization kinetics from experimental laboratory data

**Lorenzo Fusi, Alessandro Monti & Mario
Primicerio**

Journal of Mathematical Chemistry

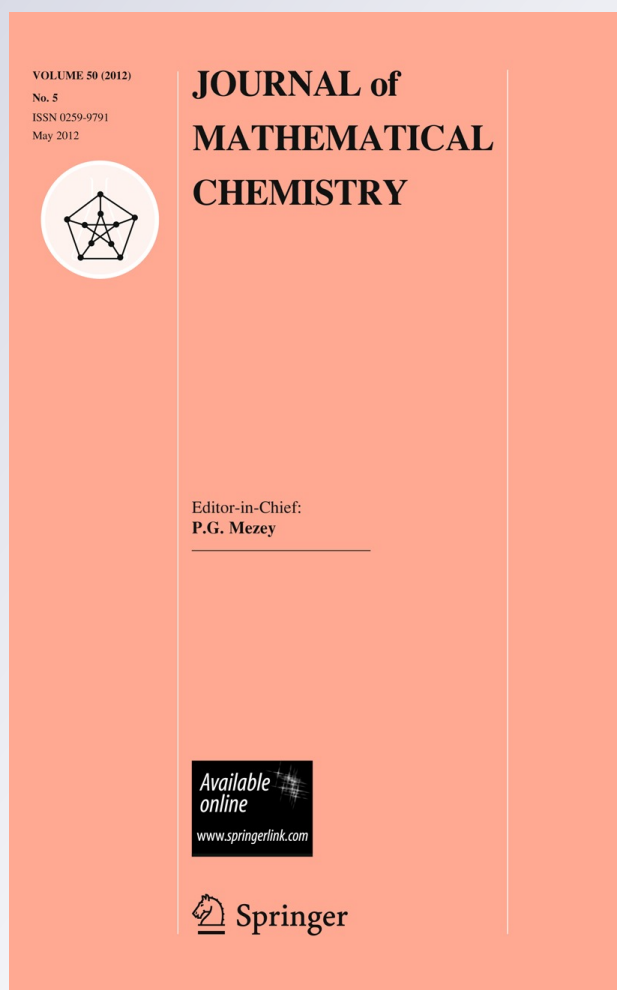
ISSN 0259-9791

Volume 50

Number 9

J Math Chem (2012) 50:2492-2511

DOI 10.1007/s10910-012-0045-3



Your article is protected by copyright and all rights are held exclusively by Springer Science+Business Media, LLC. This e-offprint is for personal use only and shall not be self-archived in electronic repositories. If you wish to self-archive your work, please use the accepted author's version for posting to your own website or your institution's repository. You may further deposit the accepted author's version on a funder's repository at a funder's request, provided it is not made publicly available until 12 months after publication.

Determining calcium carbonate neutralization kinetics from experimental laboratory data

Lorenzo Fusi · Alessandro Monti ·
Mario Primicerio

Received: 10 April 2012 / Accepted: 9 June 2012 / Published online: 22 June 2012
© Springer Science+Business Media, LLC 2012

Abstract In the framework of a research aimed at estimating the performance and lifetime of porous filters filled with marble powder and used to neutralize acid waters, we propose a mathematical model for determining the calcium carbonate reaction kinetics from some experimental data. In particular we show how to determine the order of the reaction and the reaction rate when calcium carbonate is immersed in a HCl solution. These parameters are evaluated by means of a fitting procedure based on least square methods. The experiments are performed using CaCO_3 in the form of a slab and powder and measuring (by means of BET analysis) the specific reaction surface.

Keywords Neutralization · Mathematical modelling · Calcium carbonate · Reaction kinetics

1 Introduction

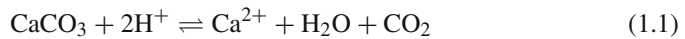
The calcium carbonate neutralization kinetics can play a key role in the acid mine drainage remediation. Acid mine drainage (AMD) or Acid rock drainage (ARD) represents a serious environmental hazard all around the world, especially since it can cause long term damages to waterways and biodiversity. AMD is mainly originated by

L. Fusi (✉) · A. Monti · M. Primicerio
Dipartimento di Matematica “Ulisse Dini”, Università degli Studi di Firenze,
Viale Morgagni 67/A, 50134 Florence, Italy
e-mail: fusi@math.unifi.it

A. Monti
I2T3, Innovazione Industriale Tramite Trasferimento Tecnologico Associazione Onlus,
Polo Scientifico Sesto Fiorentino (FI), Via Madonna del Piano 6, c/o Incubatore Universitario,
50019 Sesto Fiorentino, FI, Italy

the exposition of sulfide ores, chiefly iron pyrite, to water and oxygen and it generally refers to the generation of acid streams from abandoned mines. The consequences of AMD can be tremendous for aquatic life, the first one to come into contact with the acid outflow; the extinction of entire fish population has been repeatedly reported, but the danger occurs also for plants, animals and human beings living along the acid stream (see [1–5]).

AMD remediation can be performed by means of a wide range of techniques based on chemical and/or biological mechanisms. Among them, calcium carbonate neutralization is one of the most employed due to low costs and application easiness (see [6–10]). The overall reaction between the acid stream and calcium carbonate can be summarized as:



Calcium carbonate can be added directly to the acid water or otherwise the water can be forced through the basic bulk, in order to raise the pH of the solution; the process also triggers the oxidation and precipitation of the dissolved heavy metals as hydroxides. However, in order to optimize the use of calcium carbonate at its full potential as a remediation agent, it is necessary to have a deep knowledge of the kinetic behavior of CaCO_3 in the specific acid environment in which it will be employed. The aim of the present work is precisely the kinetic characterization of calcium carbonate neutralization process, by means of a mathematical model based on experimental data. Three kinds of experiments have been performed for the model development:

- pH evolution assessment of an acid solution reacting with a slab of CaCO_3
- pH evolution assessment of an acid solution containing a suspension of CaCO_3 powder
- measurement of the specific surface area of calcium carbonate substrates, acid treated and untreated

The model solution mimics the typical AMD, while volume and stirring conditions are varied in such a way to allow the assessment of diffusion effects.

2 The general mathematical model

The general equation (see [11–13]) that describes the evolution of the H^+ ions concentration reacting with the neutralizing calcium carbonate is given by¹

$$\frac{dc^*}{dt^*} = -k^* S^* (c^* - c_o^*)^\gamma, \quad (2.1)$$

where k^* is the so-called “rate” of the reaction, S^* is the surface available for the reaction, γ is the order of the reaction, t^* is time, c^* is the molar concentration of ions at the reacting surface and c_o^* is some threshold concentration below which the

¹ Throughout this paper the suffix * stands for dimensional quantities.

solution can be considered neutral and the reaction stops. In general the reacting surface S^* is a function of c^* and time t^* and therefore another differential equation for S^* must be provided. Of course the structure of this differential equation will depend on the geometry of the reacting medium (irregular, symmetrical, planar, etc.), so that for some particular geometries this can be easily inferred. Moreover also the rate k^* can be a function of c^* , but within reasonable variations of c^* it can be considered constant (see [12, 13]).

The constant k^* represents the rate at which the reaction occurs, giving a measure of how fast H^+ ions are neutralized by $CaCO_3$. The dimension of k^* are

$$[k^*] = \frac{1}{(surf \cdot time)} \text{ when } \gamma = 1 \quad \text{and} \quad [k^*] = \frac{conc^{1-\gamma}}{(surf \cdot time)} \text{ when } \gamma \neq 1. \quad (2.2)$$

Hence k^* measures the velocity (per unit surface) at which calcium carbonate reacts with H^+ ions. In this paper we are interested in determining the two main physical parameters entering the model, namely k^* and γ . We will derive such values using model (2.1) and exploiting data obtained from experiments in which an acid solution is neutralized using calcium carbonate in different forms (slab, powder, cubes) and also through the so-called BET analysis, which provides the specific reacting surface as a function of time. We shall see that the reaction is essentially of order one and that, in the cases of practical interest, the rate k^* is essentially constant. Equation (2.1) can be rewritten in terms of pH

$$\frac{dpH}{dt^*} = \frac{k^* S^*}{\ln 10 \times 10^{-pH}} (10^{-pH} - 10^{-pH_o})^\gamma, \quad (2.3)$$

where

$$pH = -\log_{10}(c^*). \quad (2.4)$$

3 Determining the rate constant k^* with a fixed reaction surface

In this section we determine k^* exploiting some laboratory measurements of pH at different times using a reacting surface of fixed area. To this aim we have performed simple experiments in which a slab of calcium carbonate is placed at the bottom of a beaker filled with HCl with an initial pH = pH_{in} . The experiments have been performed starting with a strongly acid solution ($pH_{in} = 2.18$) that is continuously stirred during the experiments. The pH of the solution is monitored as a function of time and the experiment is stopped when a fixed “target” pH = pH_{end} is reached. The advantage of this particular geometry is that the surface reacting with the acid water can be considered to be approximatively constant throughout the experiment.

We integrate (2.1) making the following assumption

- (A1) k^* is constant throughout the process;
- (A2) S^* is constant because of the particular plane geometry of the experiments;

(A3) The surface concentration [appearing in the r.h.s. of (2.1)] coincides with the bulk concentration that is monitored during the experiment;

Under these assumptions (2.1) [or equivalently (2.3)] can be integrated starting from a given initial condition $c^*(0) = c_{in}^*$ [or $\text{pH}(0) = \text{pH}_{in}$] obtaining immediately

$$c^* = c_o^* + \left[(c_{in}^* - c_o^*)^{1-\gamma} - (1-\gamma)t^*k^*S^* \right]^{\frac{1}{1-\gamma}}, \quad \gamma \neq 1, \tag{3.1}$$

$$c^* = c_o^* + (c_{in}^* - c_o^*) \exp\{-k^*S^*t^*\}, \quad \gamma = 1, \tag{3.2}$$

or, in terms of pH

$$\text{pH}(t^*) = -\log_{10} \left\{ 10^{-\text{pH}_o} + \left[\left(10^{-\text{pH}_{in}} - 10^{-\text{pH}_o} \right)^{(1-\gamma)} - (1-\gamma)t^*k^*S^* \right]^{\frac{1}{1-\gamma}} \right\}, \tag{3.3}$$

$$\text{pH}(t^*) = -\log_{10} \left[10^{-\text{pH}_o} + \left(10^{-\text{pH}_{in}} - 10^{-\text{pH}_o} \right) \exp(-t^*k^*S^*) \right]. \tag{3.4}$$

To use (3.1)–(3.4) to fit the experimental data thus determining k^* and γ , we have to discuss the assumptions above. Concerning (A1), according to the literature (see [12, 13]), k^* is increasing with c^* but can be taken as a constant between $\text{pH} = 2$ and $\text{pH} = 5$.

The case of (A2) is more critical since the reacting surface cannot be assumed to coincide with the geometrical surface. Nevertheless, although S^* is slightly increasing (particularly in the early stages of the process), it can be considered as constant, but not a priori known. Thus the aim of our experiment can be the determination of

$$K^* = k^*S^*, \tag{3.5}$$

where k^* could be calculated only if an independent measure of S^* is available.

Next we pass to discuss (A3) and we confine ourselves to the case $\gamma = 1$ for the sake of simplicity. If we define

$$u^*(t) = c^*(t^*) - c_o^*, \tag{3.6}$$

$$v^*(t^*) = c_s^*(t^*) - c_o^*, \tag{3.7}$$

where c^* is the H^+ concentration in the bulk and c_s^* is its value at the reacting surface, we have

$$\frac{du^*}{dt^*} = -K^*v^*. \tag{3.8}$$

On the other hand, if we assume that the concentration is uniform in the bulk (because of stirring) and is linear in a boundary layer of width h^* , mass conservation in the bulk is expressed by

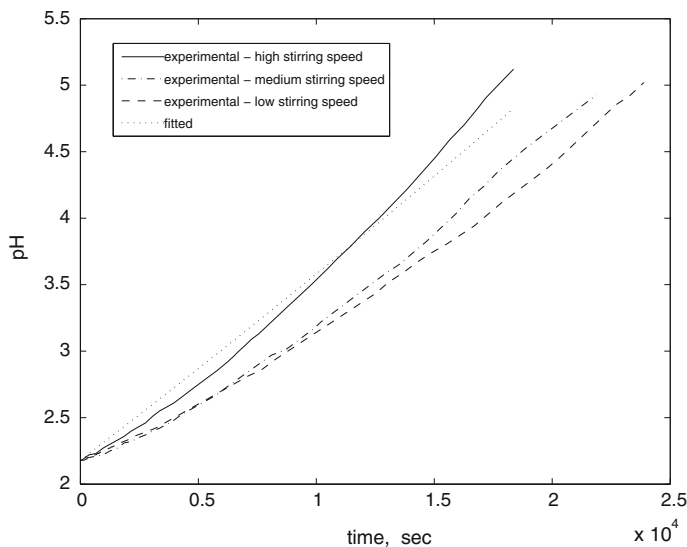


Fig. 1 Experimental pH and curve fitting: Exp 1

$$\frac{du^*}{dt^*} = -\frac{D^*}{h^*}(u^* - v^*), \tag{3.9}$$

where D^* is a constant proportional to the diffusivity coefficient (namely diffusivity per unit length). Therefore, combining (3.8) and (3.9) we get

$$\frac{du^*}{dt^*} = -\left(\frac{K^*D^*}{h^*K^* + D^*}\right)u. \tag{3.10}$$

This means that, using (3.1), (3.2) we underestimate K^* , with an error decreasing with h^* , i.e. with the increasing of the stirring speed.

Indeed, performing the experiments with increasing stirring speed, we find that the slope of the curves where pH is plotted as a function of time is increasing with the speed of the stirring. Of course, the best approximation is found by fitting the curves of largest slope.

We have performed the fitting of the curves (using least square method) in two sets different experiments (see Figs. 1, 2) and found the results

	pH_{in}	pH_{end}	γ	K^*
Exp 1	2.18	5.12	0.98 ± 0.02	$(28.30 \pm 0.3) \times 10^{-5} \left(\frac{\text{mol}}{\text{l}}\right)^{0.02} \frac{1}{\text{s}}$
Exp 2	2.15	5.5	0.96 ± 0.01	$(28.90 \pm 0.5) \times 10^{-5} \left(\frac{\text{mol}}{\text{l}}\right)^{0.04} \frac{1}{\text{s}}$

In the second experiment the volume of acid solution was one half than in the first one. For comparison we have also done an experiment with a circumneutral solution. We found the same value for γ , while the value of K^* was larger, as it is expected

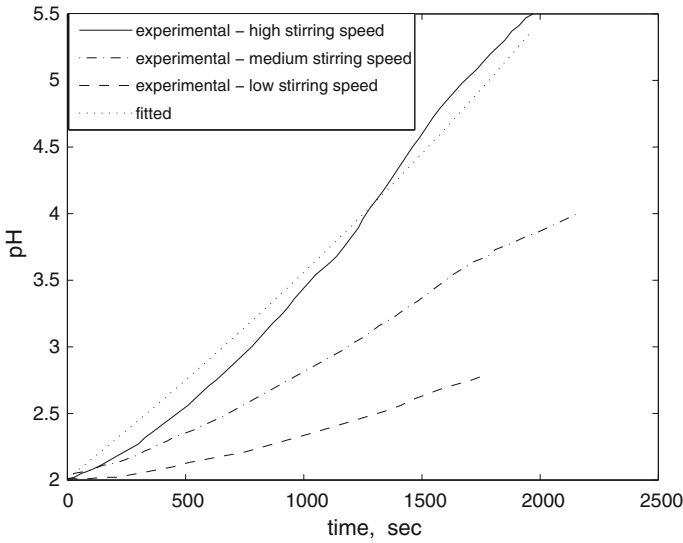


Fig. 2 Experimental pH and curve fitting: Exp 2

since the reacting surface (for an equal geometric dimensions) is expected to be much smaller because the erosion (and thus the rugosity) is much less important. Consequently we take henceforth

$$\gamma = 1. \tag{3.11}$$

As we noted above, to get an estimate for k^* we have to evaluate S^* . For this purpose we used the so-called BET analysis that is based on a theory introduced in 1938 by S. Brunauer, P.H. Emmett and E. Teller (see [14, 15]) and since then is called by the acronym of their names.

Consider the isotherm adsorption of a gas at a pressure P^* on a surface and define the following nondimensional quantities

$$\varphi = \frac{P^*}{P_o^*}, \quad \theta = \frac{V_{mono}^*}{V^*}, \tag{3.12}$$

where P_o^* is the saturation pressure, while V^* represents the volume of gas adsorbed (at pressure P^*) and V_{mono}^* represents the volume adsorbed by the surface monolayer. According to the BET theory it is

$$\theta \frac{\varphi}{1 - \varphi} = (1 - \alpha)\varphi + \alpha, \tag{3.13}$$

where α is the inverse of the so-called BET constant and can be expressed in terms of adsorption energy. Thus, measuring V^* at different pressures the quantity V_{mono}^* can be deduced and through the geometric properties of the gas, the area of the adsorbing surface can be estimated.

The analysis has been performed with a cycle of adsorption/desorption of nitrogen at 77 °K, using automatic analyzer ASAP 2010 Micromeritics. The nitrogen adsorp-

tion isotherm has been performed by means of successive controlled additions of gaseous nitrogen to the burette containing the sample; after each addition the equilibrium pressure has been measured, the saturation pressure has been evaluated every 2 h. The nitrogen desorption isotherm has been assessed after the absorption cycle, through consecutive controlled withdrawals of gaseous nitrogen from the burette containing the sample; after each withdrawal, the equilibrium pressure has been measured.

We have analyzed 26 parallelepipeds of CaCO_3 with dimensions $0.4 \times 0.8 \times 0.8$ cm that had been immersed in a solution whose pH is increased from $\text{pH} \approx 2$ to $\text{pH} \approx 4$. The time needed to reach the pH target was 22 min and the solution has been kept stirred (720 rpm). We have obtained that the total reacting surface was $5453 \pm 72 \text{ cm}^2$ whereas the geometrical surface was 66.5 cm^2 . Thus, the ratio between the two surfaces is 81.92 ± 1.08 . This means that in the experiments 1 and 2

$$S^* \approx (1.061 \pm 0.014) \times 10^3 \text{ cm}^2, \tag{3.14}$$

so we get the following estimated value of k^*

$$k^* = (2.67 \pm 0.06) \times 10^{-7} \frac{1}{\text{cm}^2 \cdot \text{s}} \quad \text{Exp 1.} \tag{3.15}$$

$$k^* = (2.73 \pm 0.08) \times 10^{-7} \frac{1}{\text{cm}^2 \cdot \text{s}} \quad \text{Exp 2.} \tag{3.16}$$

4 Determining the rate constant k^* with an evolving reaction surface

Another series of experiments was performed using marble powder as the neutralizing agent. We used 12 g of CaCO_3 powder uniformly distributed in 1.8 l of an acid solution. The powder is so fine that gravity settling does not occur and the boundary layer is negligible. On the other hand, in this case the reacting surface is not constant since the marble particles are consumed during the process.

The experiments were performed in the following way

- (i) A fixed amount of CaCO_3 powder is immersed in a fixed volume V^* of HCl until a target pH_1 is reached at some time t_1^* . Then the powder is filtrated and the residual mass is dried, weighted and sent to BET analysis, which provides $S^*(t_1^*)$.
- (ii) The same amount of powder is again immersed in the same volume of HCl but now the experiment is stopped at some time $t_2^* > t_1^*$ corresponding to $\text{pH}_2 > \text{pH}_1$. Once again the residual CaCO_3 is dried, weighted and analyzed through BET, providing $S^*(t_2^*)$ and so on until the pH target is reached.

Now (2.1), where—according to the discussion of the previous section—we set $\gamma = 1$, gives

$$c^* = c_o^* + (c_{in}^* - c_o^*) \exp \left[-k^* \int_0^{t^*} S^*(\tau^*) d\tau^* \right] \tag{4.1}$$

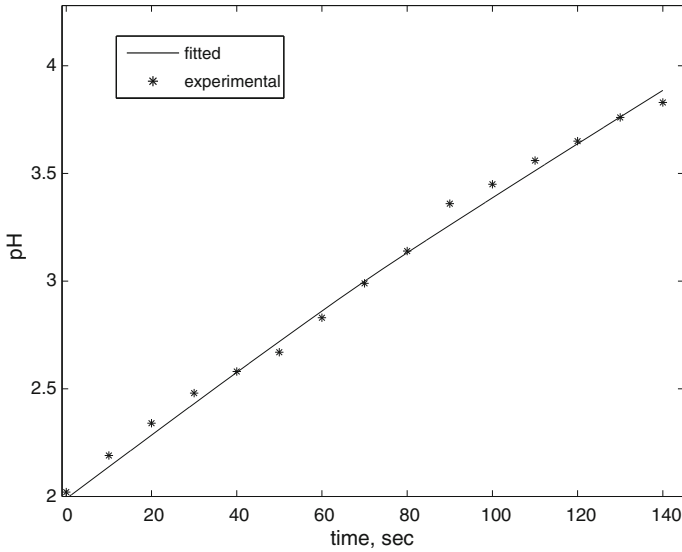


Fig. 3 Exp 1: fitting of k^* by means of (4.2)

$$pH(t^*) = -\log_{10} \left[10^{-pH_o} + (10^{-pH_{in}} - 10^{-pH_o}) \exp \left(-k^* \int_0^{t^*} S^*(\tau^*) d\tau^* \right) \right]. \tag{4.2}$$

Having the data for $pH(t^*)$ and for $S^*(t^*)$ we can obtain k^* as a result of a simple fitting procedure. The experimental conditions are the following

	pH_{in}	pH_{end}
Exp 1	2.07	3.76
Exp 2	2.15	3.98
Exp 3	2.18	5.05

and the curve fitting (Figs. 3, 4, 5) by means of (4.2) is easily performed. In Fig. 6 the function $S^* = S^*(t^*)$ is shown. The curve is obtained interpolating (using piecewise cubic Hermite polynomial) the experimental BET data at different times. Consequently we have the following

	k^*
Exp 1	$(2.7 \pm 0.2) \times 10^{-7} \text{ cm}^{-2} \cdot \text{s}^{-1}$
Exp 2	$(3.1 \pm 0.2) \times 10^{-7} \text{ cm}^{-2} \cdot \text{s}^{-1}$
Exp 3	$(3.3 \pm 0.4) \times 10^{-7} \text{ cm}^{-2} \cdot \text{s}^{-1}$

The results agree with the results of the previous section [see (3.16)] where we anticipated that the constant k^* could be underestimated because of the approximation of assumption (A3).

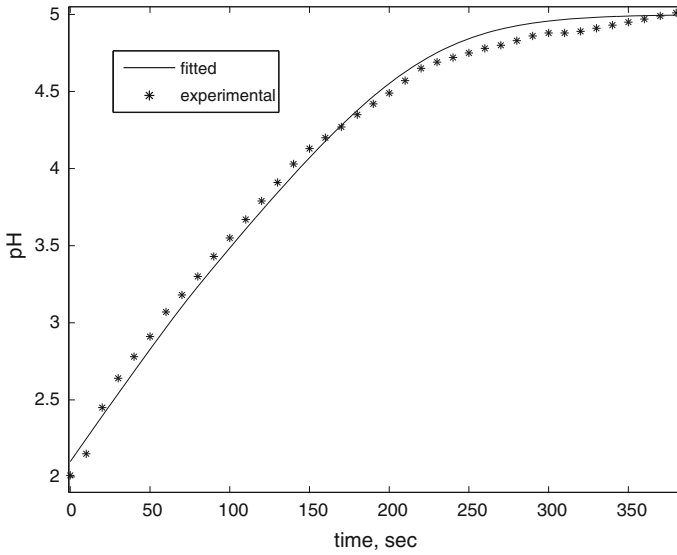


Fig. 4 Exp 2: fitting of k^* by means of (4.2)

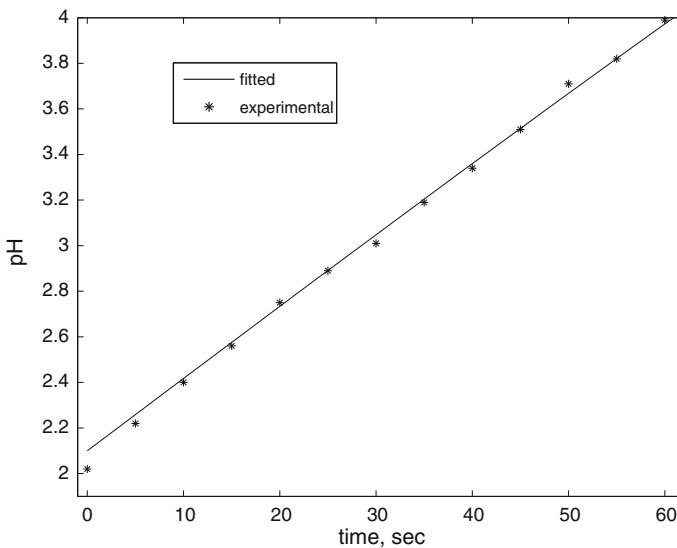


Fig. 5 Exp 3: fitting of k^* by means of (4.2)

5 The ideal case of spherical particles

In this section we develop a simple mathematical model for the experimental setting of the previous section (marble powder suspended in an acid solution), but making the additional simplifying assumption that the powder is made of N spherical particles of the same radius.

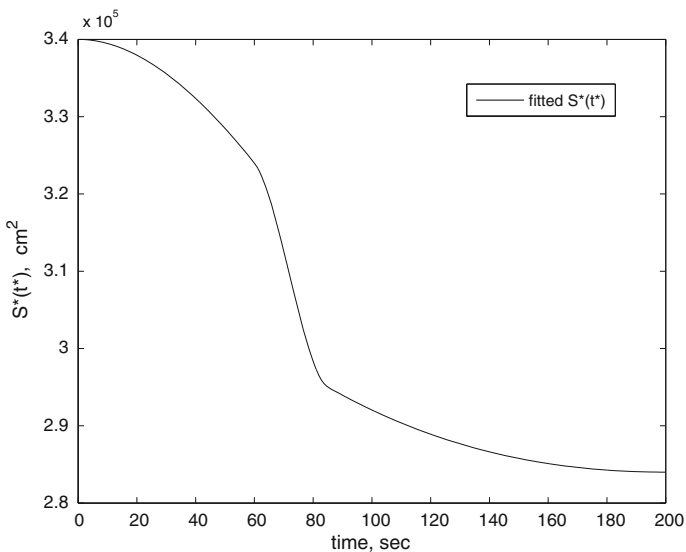


Fig. 6 Plot of the function $S^* = S^*(t^*)$ interpolating the BET experimental data

Of course, applying this model will not give us a precise evaluation of k^* , but since the estimates that will be obtained are of the same order of magnitude of the results of Sects. 3 and 4, we will infer that this ideal situation is not too far from giving realistic results.

We take a volume V^* of acid HCl solution and suppose that N spheres of CaCO_3 are immersed in such a volume. Molar mass balance implies that the rate at which moles (per unit volume) of H^+ ions are neutralized is twice the rate at which moles (per unit volume) of CaCO_3 are consumed. As before we denote by c^* the acid molar concentration (mol/Vol), by S^* the total reacting surface of the spheres, by r^* the radius of the single sphere and by ρ^* the molar density (mol/Vol) of the spheres. Assuming spatial homogeneity (diffusion is neglected and all the main variables depend only on time t^* , as in the case of a stirred solution) we have

$$\frac{d}{dt^*}(2c^*V^*) = \frac{d}{dt^*}\left(\frac{4N\rho^*\pi r^{*3}}{3}\right), \tag{5.1}$$

where the coefficient 2 on the l.h.s is due to the stoichiometric coefficient in the l.h.s of (1.1). From (5.1)²

$$2V^*\frac{dc^*}{dt^*} = 4N\rho^*\pi r^{*2}\frac{dr^*}{dt^*}. \tag{5.2}$$

² The volume V^* is supposed to be sufficiently larger than the volume occupied by CaCO_3 (as in the case of the experiments considered in this paper), so that it can be treated as a constant.

We still assume that the reaction kinetics is of the type (2.1) and write

$$-\frac{dc^*}{dt^*} = k^* S^* (c^* - c_o^*)^\gamma = k^* 4N\pi r^{*2} (c^* - c_o^*)^\gamma, \tag{5.3}$$

Plugging (5.3) into (5.2) we get the evolution equation for r^*

$$-\frac{dr^*}{dt^*} = \left(\frac{2k^* V^*}{\rho^*}\right) (c^* - c_o^*)^\gamma. \tag{5.4}$$

The system is therefore governed by the following set of ODE's

$$\begin{cases} -\frac{dc^*}{dt^*} = k^* 4N\pi r^{*2} (c^* - c_o^*)^\gamma, & c^*(0) = c_{in}^*, \\ -\frac{dr^*}{dt^*} = \left(\frac{2k^* V^*}{\rho^*}\right) (c^* - c_o^*)^\gamma, & r^*(0) = r_{in}^*, \end{cases} \tag{5.5}$$

where c_{in}^* and r_{in}^* represent the molar acid initial concentration and the spheres initial radius respectively. Clearly we suppose that $c_{in}^* > c_o^*$, otherwise the solution would be already neutralized. We rescale the variables in the following manner

$$c = \frac{c^*}{c_o^*}, \quad r = \frac{r^*}{r_{in}^*}, \quad t = \frac{t^*}{t_o^*}, \tag{5.6}$$

where t_o^* is a characteristic time to be selected. The nodimensional formulation of (5.5) is

$$\begin{cases} -\frac{dc}{dt} = \left(\frac{t_o^*}{t_H^*}\right) r^2 (c - 1)^\gamma, & c(0) = c_{in}, \\ -\frac{dr}{dt} = \left(\frac{t_o^*}{t_s^*}\right) (c - 1)^\gamma, & r(0) = 1. \end{cases} \tag{5.7}$$

where t_H^* e t_s^* are the reaction and consumption characteristic times

$$t_H^* = \frac{1}{4N\pi r_{in}^{*2} k^* c_o^{*\gamma-1}}, \quad t_s^* = \frac{\rho^* r_{in}^*}{2k^* V^* c_o^{*\gamma}}, \tag{5.8}$$

and where $c_{in} = c_{in}^*/c_o^* > 1$. We select $t_o^* = t_s^*$ (consumption characteristic time). From (5.7)₁ it is easy to see that

$$(c(t) - 1)^{1-\gamma} = (c_{in} - 1)^{1-\gamma} - (1 - \gamma) \int_0^t \left(\frac{t_s^*}{t_H^*}\right) r^2(\tau) d\tau, \quad \gamma \neq 1, \tag{5.9}$$

and

$$c(t) = 1 + (c_{in} - 1) \exp \left\{ - \left(\frac{t_s^*}{t_H^*} \right) \int_0^t r^2(\tau) d\tau \right\}, \quad \gamma = 1. \quad (5.10)$$

System (5.7) can also be rewritten as

$$\begin{cases} \frac{dc}{dr} = \left(\frac{t_s^*}{t_H^*} \right) r^2, \\ c(1) = c_{in}, \end{cases} \quad (5.11)$$

and hence we can write c as a function of the radius r

$$c(r) = c_{in} + \frac{1}{3} \left(\frac{t_s^*}{t_H^*} \right) (r^3 - 1). \quad (5.12)$$

Remark 5.1 The ratio of the characteristic times is given by

$$\frac{t_s^*}{t_H^*} = \frac{4N\pi r_{in}^{*3} \rho^*}{2V^* c_o^*} =: \frac{3N_{in}^s}{2N_o^H}, \quad (5.13)$$

where

$$N_{in}^s = \frac{4}{3} N\pi r_{in}^{*3} \rho^*, \quad (5.14)$$

is the overall initial number of CaCO_3 moles and

$$N_o^H = V^* c_o^*, \quad (5.15)$$

is the number of acid moles when the concentration c_o^* is reached (neutralized solution). We notice that such a ratio does not depend on γ and k^* .

Remark 5.2 Recalling that $c_{in} > 1$ it is easy to show that, from (5.9), (5.10), $c > 1$.

5.1 Reaction of order $\gamma = 1$

If the order of the reaction is 1, the adimensional concentration is given by (5.10), while the concentration as a function of the radius is given by (5.12). From (5.10) it is evident that complete neutralization ($c = 1$) cannot be reached in a finite time. Moreover, looking at (5.12), if the spheres disappear in a finite time then the concentration becomes

$$c = c_{in} - \frac{1}{3} \left(\frac{t_s^*}{t_H^*} \right). \quad (5.16)$$

Recalling that $c > 1$ (see Remark 5.2), the condition ensuring the complete consumption of the spheres is

$$c_{in} - \frac{1}{3} \left(\frac{t_s^*}{t_H^*} \right) > 1. \tag{5.17}$$

Therefore when (5.17) holds, the reactant is depleted in a finite time. When $\gamma = 1$ the system of ODE's (5.7) can be integrated to get an explicit expression for $t(r)$. Indeed, from (5.7)₂ (with $\gamma = 1$) and (5.12), we have

$$-\frac{dt}{dr} = \frac{1}{A^3 r^3 - B^3}, \tag{5.18}$$

where

$$A^3 =: \frac{1}{3} \left(\frac{t_s^*}{t_H^*} \right), \quad B^3 =: \left[1 + \frac{1}{3} \left(\frac{t_s^*}{t_H^*} \right) \right] - c_{in} = A^3 + (1 - c_{in}). \tag{5.19}$$

After some algebra

$$-3B \frac{dt}{dr} = \left[\frac{1}{B} \frac{1}{Ar - B} - \frac{(A/B)r + 2}{A^2 r^2 + ABr + B^2} \right], \tag{5.20}$$

whose integration between 1 and r provides $t(r)$

$$t(r) = \frac{1}{3AB^2} \left\{ \ln \left[\frac{|A - B|}{|Ar - B|} \cdot \frac{\sqrt{|A^2 r^2 + ABr + B^2|}}{\sqrt{|A^2 + AB + B^2|}} \right] + \sqrt{3} \arctan \left(\frac{2Ar + B}{\sqrt{3}B} \right) - \sqrt{3} \arctan \left(\frac{2A + B}{\sqrt{3}B} \right) \right\} \tag{5.21}$$

From (5.19), we notice that, when $B > 0$, spheres are not depleted while, when $B = 0$ depletion occurs in an infinite time. The case $B < 0$ corresponds to depletion in a finite time. In particular, when $B < 0$, the depletion time t_d is obtained setting $r = 0$ in (5.21)

$$t_d = \frac{1}{3AB^2} \left[\ln \frac{|A - B|}{|B|} \cdot \frac{\sqrt{|B^2|}}{\sqrt{|A^2 + AB + B^2|}} + \sqrt{3} \arctan \left(\frac{1}{\sqrt{3}} \right) - \sqrt{3} \arctan \left(\frac{2A + B}{\sqrt{3}B} \right) \right]. \tag{5.22}$$

From (5.12) we see that the concentration at time t_d is

$$c_d = c_{in} - \frac{1}{3} \left(\frac{t_s^*}{t_H^*} \right) = c_{in} - A^3 = 1 - B^3 > 1 \tag{5.23}$$

When $B > 0$ the radius of each sphere tends to $r_{end} > 0$ and this limit is obtained setting $c = 1$ in (5.12)

$$r_{end} = \sqrt[3]{1 + (1 - c_{in}) \frac{3t_H^*}{t_s^*}} = \frac{B}{A} > 0. \tag{5.24}$$

When $B = 0$ we have $r_{end} = 0$.

5.2 Reaction of order $\gamma \neq 1$

When the reaction rate is different from 1, we cannot obtain an explicit expression for $t(r)$. Indeed from (5.7)

$$-\frac{dt}{dr} = \frac{1}{[A^3 r^3 - B^3]^\gamma}. \tag{5.25}$$

Integrating (5.25) between r and 1 we get

$$t(r) = \int_r^1 \frac{d\xi}{[A^3 \xi^3 - B^3]^\gamma}. \tag{5.26}$$

Analogously to the previous case, when $B < 0$ the function $t(r)$ is bounded and the spheres are consumed in the finite time

$$t_d = t(0) = \int_0^1 \frac{d\xi}{[A^3 \xi^3 - B^3]^\gamma}, \tag{5.27}$$

with concentration at $t = t_d$ [see again (5.12)] given by

$$c_d = c_{in} - \frac{1}{3} \left(\frac{t_s^*}{t_H^*} \right) = c_{in} - A^3 = 1 - B^3 > 1 \tag{5.28}$$

We can show that when $B > 0$ the radius tends to $r_{end} = B/A \in (0, 1)$ and in case $B = 0$ we have $r_{end} = 0$. In both cases the radius r_{end} is reached in a finite or infinite time depending on γ . From the definition of B and A , when $B > 0$, it is easy to check that $0 < B/A < 1$ [see (5.19)]. Let us then consider

$$t\left(\frac{B}{A}\right) = \int_{\frac{B}{A}}^1 \frac{d\xi}{[A^3 \xi^3 - B^3]^\gamma}. \tag{5.29}$$

Introducing the new variable

$$z = \xi^3 - \left(\frac{B}{A}\right)^3, \tag{5.30}$$

integral (5.29) becomes

$$t\left(\frac{B}{A}\right) = \frac{1}{3A^{3\gamma}} \int_0^{1-\left(\frac{B}{A}\right)^3} \frac{dz}{\left[z + \left(\frac{B}{A}\right)^3\right]^{2/3} z^\gamma}. \tag{5.31}$$

Since

$$\left(\frac{B}{A}\right)^3 \leq z + \left(\frac{B}{A}\right)^3 \leq 1, \tag{5.32}$$

we have that

$$\frac{1}{3A^{3\gamma}} \int_0^{1-\left(\frac{B}{A}\right)^3} \frac{dz}{z^\gamma} \leq t\left(\frac{B}{A}\right) \leq \frac{A^2}{3A^{3\gamma} B^2} \int_0^{1-\left(\frac{B}{A}\right)^3} \frac{dz}{z^\gamma}. \tag{5.33}$$

Therefore from the theory on improper integrals

- $\gamma < 1,$ \iff $t(B/A) < \infty,$
- $\gamma \geq 1,$ \iff $t(B/A) = \infty.$

This means that, when $B > 0$ and $\gamma < 1$ the radius of the spheres tends to $r_{end} = B/A \in (0, 1)$ in a finite time. On the other hand, when $\gamma > 1$, the radius of the spheres tends $r_{end} = B/A \in (0, 1)$ in an infinite time.

Remark 5.3 We notice that, in case $\gamma < 1$, at time $t = t(B/A)$ we have $r = B/A$ and hence, from (5.25), $dr/dt = 0$, implying $c = 1$ (complete neutralization is reached). In case $\gamma \geq 1$ complete neutralization is reached in an infinite time.

When $B = 0$ (which is a very peculiar case) we have a slightly different situation. Clearly $r_{end} = 0$ and from (5.29)

$$t(0) = \int_0^1 \frac{d\xi}{A^{3\gamma} \xi^{3\gamma}} = \begin{cases} \frac{1}{A^{3\gamma}} \left. \frac{\xi^{1-3\gamma}}{1-3\gamma} \right|_0^1 = \frac{1}{A^{3\gamma}} < \infty, & \gamma < \frac{1}{3}, \\ +\infty, & \gamma \geq \frac{1}{3}. \end{cases} \tag{5.34}$$

Summarizing we can get the following scheme

- Case (I), $B < 0, \iff r = 0, c = c_d > 1,$ (from 5.28),
 $t = t_d,$ (from 5.27)
- Case (II), $B > 0, \gamma \geq 1, \iff r = r_{end}, c = 1, t = t \left(\frac{B}{A} \right) = \infty,$
- Case (IIbis), $B > 0, \gamma < 1, \iff r = r_{end}, c = 1, t = t \left(\frac{B}{A} \right) < \infty,$
- Case (III), $B = 0, \gamma \geq 1/3, \iff r = 0, c = 1, t = t \left(\frac{B}{A} \right) = \infty,$
- Case (IIIbis), $B = 0, \gamma < 1/3, \iff r = r_{end}, c = 1, t = \frac{1}{A^{3\gamma}} < \infty.$

In (IIbis) the neutralization time can be estimated from (5.33) and numerically calculated from (5.29). Of course all these cases can be rewritten also for the dimensional variables.

Let us define \bar{m}^* as the total mass of CaCO_3 at some time and let \bar{S}^* be the specific surface (surface per unit mass) provided by the BET analysis so that

$$\bar{m}^* = \frac{4}{3}\pi \bar{r}^{*3} N \hat{\rho}^*, \tag{5.35}$$

$$\bar{m}^* \cdot \bar{S}^* = 4\pi \bar{r}^{*2} N, \tag{5.36}$$

where $\hat{\rho}^*$ is CaCO_3 density³ and \bar{r}^* is the radius of the spheres at the same time. Dividing (5.35) by (5.36) we get

$$\bar{r}^* = \frac{3}{\bar{S}^* \hat{\rho}^*}, \tag{5.37}$$

which inserted into (5.35) or into (5.36) provides the number

$$N = \frac{\bar{m}^* \cdot \bar{S}^{*3} \cdot \hat{\rho}^{*2}}{36\pi}. \tag{5.38}$$

This means that the radius of the particles at any time $r^*(t^*)$ can be calculated in terms of the mass of the marble powder $m^*(t^*)$ measured at the same time:

$$r^*(t^*) = \bar{r}^* \sqrt[3]{\frac{m^*(t^*)}{\bar{m}^*}}. \tag{5.39}$$

³ The density $\hat{\rho}^*$ represents mass per unit volume of CaCO_3 (typically $\approx 2.7 \text{ g/cm}^3$). Denoting with \mathcal{M}_s the molecular weight of CaCO_3 ($\mathcal{M}_s \approx 100 \text{ g/mol}$) the relation between molar density and density is $\hat{\rho}^* = \mathcal{M}_s \rho^*$.

From the knowledge of V^* (which we recall has been taken sufficiently large⁴) and from the knowledge of c_o^* we can now determine the characteristic times

$$t_H^* = \frac{1}{4N\pi r_{in}^{*2} k^* c_o^{*\gamma-1}}, \quad t_s^* = \frac{\rho^* r_{in}^*}{2k^* V^* c_o^{*\gamma}}, \quad (5.40)$$

where k^* , γ have to be found and where we recall that the ratio t_s^*/t_H^* does not depend on k^* [see (5.13)]. The adimensional constants A and B [not depending on k^* , γ , see (5.19)] are thus obtained and we determine the function $t(r)$ by means of (5.26), i.e.

$$t(r) = \int_r^1 \frac{d\xi}{[A^3 \xi^3 - B^3]^\gamma}. \quad (5.41)$$

Recalling that $r(t)$ is strictly monotone (decreasing) we can build the inverse of (5.41), namely $r(t)$. Then we plug this function into (5.12) and we get the concentration as a function of time and hence the function $\text{pH}(t)$. Now we must compare the plot of $\text{pH}(t)$ obtained from the model with the experimental one. Since $\text{pH}(t^*) = \text{pH}(t_s^*)$, we fit the rate constant k^* and the order of the reaction γ through the dimensional characteristic time t_s^* [see (5.40)]. In what follows we show the results of three experiments. In all the experiments $c_o^* = 7.9433 \times 10^{-11} \text{ mol/cm}^3$, which corresponds to $\text{pH} = 7.1$. In what follows m_{in}^* , m_{end}^* denote the initial and final mass, whereas r_{in}^* , r_{end}^* the initial and final radii.

5.2.1 Example 1

In this experiment we have

$$m_{in}^* = 12.18 \text{ g}, \quad m_{end}^* = 12.00 \text{ g}, \quad \hat{\rho} = 2.7 \text{ g/cm}^3, \quad V^* = 1800 \text{ cm}^3 \quad (5.42)$$

$$S^* = 2.7 \times 10^{-4} \text{ cm}^2/\text{g}, \quad \text{pH}_o = 7.1, \quad \text{pH}_{in} = 2.02, \quad \text{pH}_{end} = 3.99, \quad (5.43)$$

implying

$$c_{in}^* = 9.5499 \times 10^{-6} \text{ mol/cm}^3, \quad N = 1.5225 \times 10^{13} \quad (5.44)$$

$$r_{in}^* = 4.1357 \times 10^{-5} \text{ cm}, \quad r_{end}^* = 4.1152 \times 10^{-5} \text{ cm}. \quad (5.45)$$

In this case the values for k^* , γ are (see Fig. 7)

$$k^* = 2.15 \times 10^{-7} \frac{1}{\text{s} \cdot \text{cm}^2}, \quad \gamma = 0.95. \quad (5.46)$$

⁴ In the experiments the ratio between the water volume and the volume occupied by CaCO_3 spheres is $O(10^{-3})$.

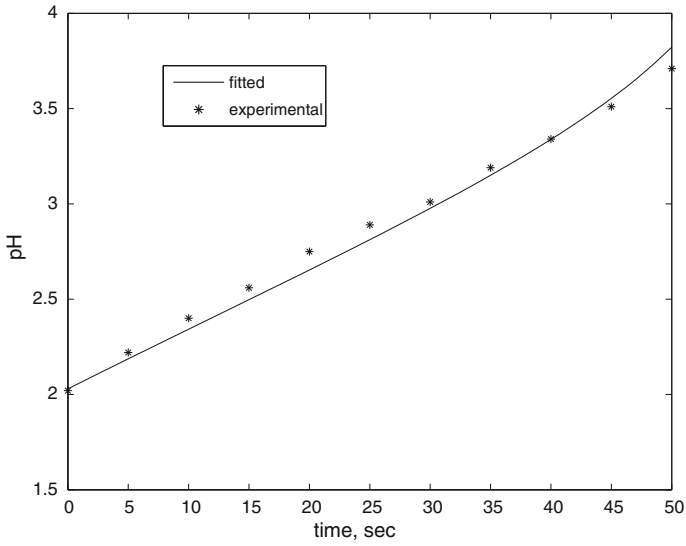


Fig. 7 Example 1. Fitting of k^*

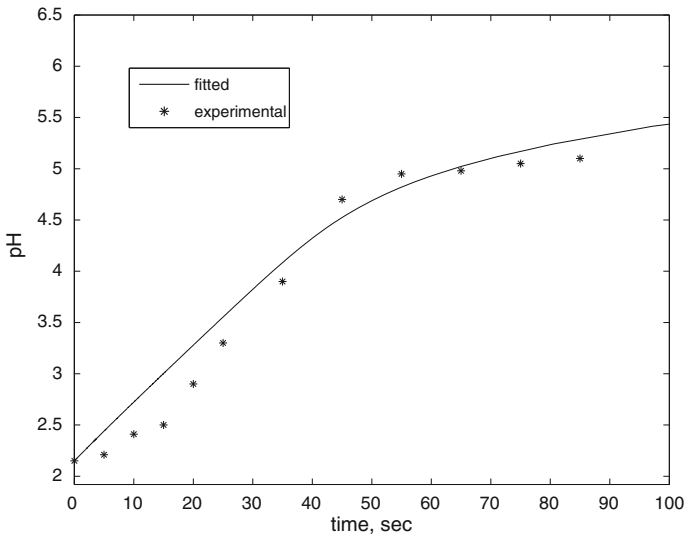


Fig. 8 Example 2. Fitting of k^*

5.3 Example 2

In this experiment we have

$$m_{in}^* = 12.18 \text{ g}, \quad m_{end}^* = 11.83 \text{ g}, \quad \hat{\rho} = 2.7 \text{ g/cm}^3, \quad (5.47)$$

$$S^* = 2.5 \times 10^{-4} \text{ cm}^2/\text{g}, \quad \text{pH}_o = 7.1, \quad \text{pH}_{in} = 2.15, \quad \text{pH}_{end} = 5.10, \quad (5.48)$$

implying

$$c_{in}^* = 7.0795 \times 10^{-6} \text{ mol/cm}^3, \quad N = 1.1915 \times 10^{13} \quad (5.49)$$

$$r_{in}^* = 4.4878 \times 10^{-5} \text{ cm}, \quad r_{end}^* = 4.4444 \times 10^{-5} \text{ cm}. \quad (5.50)$$

In this case k^* , γ are (see Fig. 8)

$$k^* = 4.3 \times 10^{-7} \frac{1}{s \cdot \text{cm}^2}, \quad \gamma = 0.97. \quad (5.51)$$

As we can see, although the assumption of monogranular powder is completely unrealistic, the results are in the same range of the ones evaluated in the real situation.

Acknowledgments The present work has been developed for the project CREA (sistema di Cartucce Reattive per gli Effluenti Acidi di miniera), funded by the Region Tuscany within the POR FESR 2007-2013 Activity 1.1 line A and B “Regional call 2008 to support joint research projects between groups of companies and research organizations in the field of environment, transport, logistics, info-mobility and energy”. We also want to express our thanks to the project team leader Massa Spin Off and especially to Dr. Massimo Rolla, for the support and collaboration in the experimental activities.

References

1. L.B. Starnes, D.C. Gasper, Effects of surface mining on aquatic resources in North America. *Fisheries* **20**, 20–23 (1995)
2. J.V. Arnekleiv, L. Storet, Downstream effects of mine drainage on benthos and fish in a Norwegian river: a comparison of the situation before and after river rehabilitation. *J. Geochem. Explor.* **52**, 35–43 (1995)
3. J.G. Wiener, J.P. Giesy, Concentrations of Cd, Cu, Mn, Pb, and Zn in fishes in a highly organic softwater pond. *J. Fish. Res. Board Can.* **36**, 270–279 (1979)
4. C.G. Norey, M.W. Brown, A. Cryer, J. Kay, A comparison of the accumulation, tissue distribution and secretion of cadmium in different species of freshwater fish. *Comp. Biochem. Physiol.* **96**, 181–184 (1990)
5. A. Suresh, B. Sivaramakrishna, K. Radhakrishnaiah, Patterns of cadmium accumulation in the organs of fry and fingerlings of freshwater fish *Cyprinus carpio* following cadmium exposure. *Chemosphere* **26**, 945–953 (1993)
6. Hedin R.J., Watzlaf G.R., Nairn R.W., Passive treatment of coal mine drainage with limestone. *J. Environ. Qual.* **23**, 1338–1345 (1994)
7. P.L. Sibrell, B.J. Watten, Evaluation of sludge produced by limestone neutralization of AMD at the Friendship Hill National Historic Site, in *Proceedings of the 20th Annual Meeting American Society for Mining and Reclamation*, Billings, Montana, (2003), pp. 1151–1169
8. N. Masuda, K. Hashimoto, H. Asano, E. Matsushima, S. Yamaguchi, Test results of a newly proposed neutralization process to reduce and utilize the sludge. *Miner. Eng.* **21**, 310–316 (2008)
9. A. Alcolea, M. Vázquez, A. Caparrós, I. Ibarra, C. García, R. Linares, R. Rodríguez, Heavy metal removal of intermittent acid mine drainage with an open limestone channel. *Miner. Eng.* **26**, 86–98 (2012)
10. S. Pepe Herrera, H. Uchiyama, T. Igarashi, K. Asakura, Y. Ochi, F. Ishizuka, S. Kawada, Acid mine drainage treatment through a two-step neutralization ferrite-formation process in northern Japan: physical and chemical characterization of the sludge. *Miner. Eng.* **20**, 1309–1314 (2007)
11. P. Barton, T. Vatanatham, Kinetics of limestone neutralization of acid waters. *Environ. Sci. Technol.* **10**(3), 262–266 (1976)
12. H. Nogami, T. Nagai, Studies on powdered preparations. VII. Acid neutralizing velocity of antacids. *Chem. Pharm. Bull.* **10**(8), 728–740 (1962)

13. R.E. Notari, T.D. Sokoloski, Kinetics of calcium carbonate neutralization. *J. Pharm. Sci.* **54**(10), 1500–1504 (1965)
14. S. Brunauer, P.H. Emmett, E. Teller, Adsorption of gases in multimolecular layers. *J. Am. Chem. Soc.* **60**, 309–319 (1938)
15. S. Brunauer, *Physical Adsorption* (Princeton University Press, Princeton, 1945)